Supplementary information

Multivalency-induced Structural Variations in 2D selenium Nanosheets: Facile solution-phase Synthesis and Optical Properties

Swathi V. M., [a] Arjun K., [b] Anju Rajan, [a] Raghu Chatanathodi, [a] Karthikeyan Balasubramanian [b] and Aji A. Anappara [a]*

[a] *Department of Physics, National Institute of Technology Calicut (NITC), Kozhikode-673601, Kerala, India. E-mail: aji@nitc.ac.in*

[b] *Nanophotonics Laboratory, Department of Physics, National Institute of Technology, Thiruchirappalli -620 015, India*

I. SEM images of bulk selenium powder

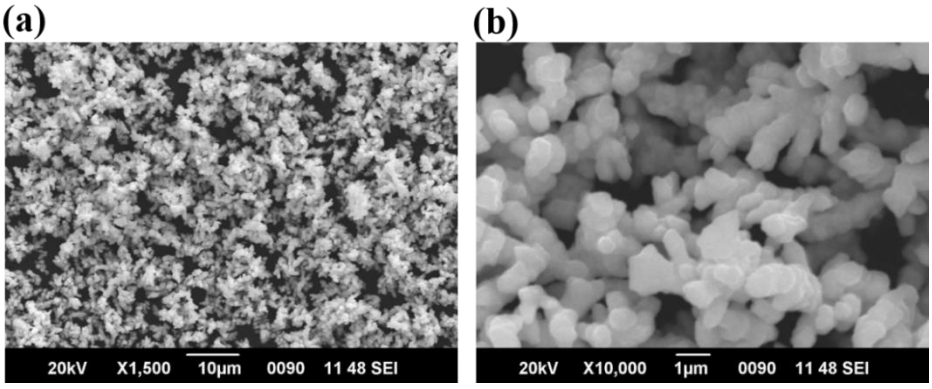

Fig.S1 SEM images of bulk selenium powder

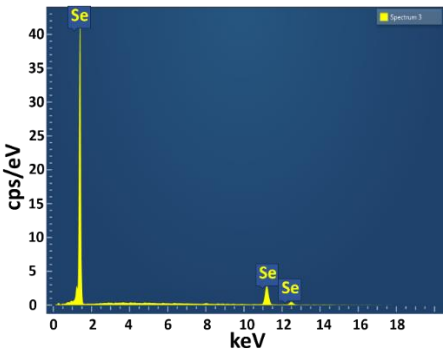

Fig.S2 SEM-EDS spectrum of bulk selenium powder.

II.X-ray Diffraction Analysis (XRD) of bulk selenium powder

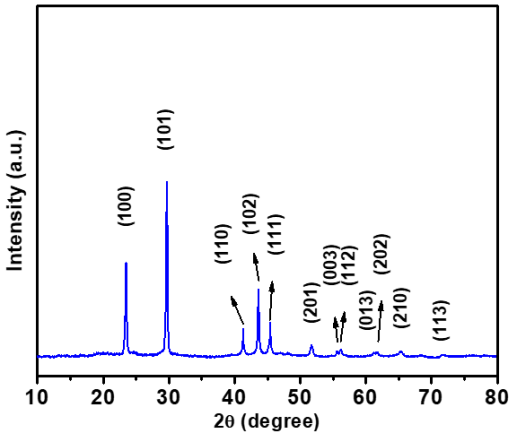

Fig.S3 X-ray diffraction (XRD) pattern of pristine selenium powder sample.

The XRD pattern verifies the crystallinity of the sample and the unit cell parameters calculated from the XRD data: 4.35 Å and 4.94 Å were found to be in good agreement with the specific (JCPDS data) values for the lattice parameters of Se: a = 4.36 Å, c = 4.96 Å. The positions of X-ray peaks (2θ values), (hkl) values and d-spacings are included in Table.I.

Bulk Se Angle (2θ)	**(hkl)**	**d-spacing (nm)**
23.57	100	3.781
29.69	011 or 101	3.009
41.40	110	2.183
43.68	012 or 102	2.076
45.48	111	1.998
51.82	201	1.767
55.60	003	1.656
56.12	112	1.640
61.27	013 or 103	1.516
61.71	202 or 022	1.504
65.28	210	1.429
71.67	113	1.319

Table.I: d-spacings from XRD data of the pristine Se powder sample.

III. Crystal structure of bulk selenium` ZXCVBNMXCV

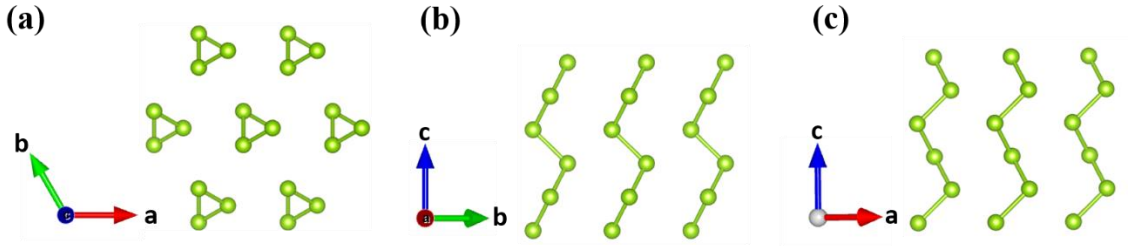

Fig.S4 (a) Top and (b) & (c) side views of bulk selenium.

All computational simulations were conducted using Density Functional Theory (DFT) as implemented in the Vienna Ab initio Simulation Package (VASP)[1,2]. We adopted the Perdew, Burke, and Ernzerhof (PBE)[3] exchange-correlation functional within the generalized gradient approximation (GGA). To account for the influence of long-range van der Waals (vdW) interactions, we employed the DFT-D2 method devised by Grimme[4] as implemented in VASP. The band gap calculations were carried out using the hybrid functional, Heyd–Scuseria–Ernzerhof (HSE06).[5] The interaction between valence electrons and frozen cores was described by the projector augmented wave (PAW) method.[6] The selenium unit cell optimization with a plane wave energy cutoff of 400 eV was subject to a $10 \times 10 \times 10$ k-point sampling, employing the Monkhorst-Pack scheme[7]. Geometry optimizations were executed with energy convergence criteria set at 10^{-4} eV and force convergence at 10^{-3} eV/Å. The unit cell parameters of selenium, optimized using the PBE functional, are $a = 4.46$Å, $c = 5.05$Å

IV. UV-visible absorption spectrum (UV-DRS) of pristine selenium powder

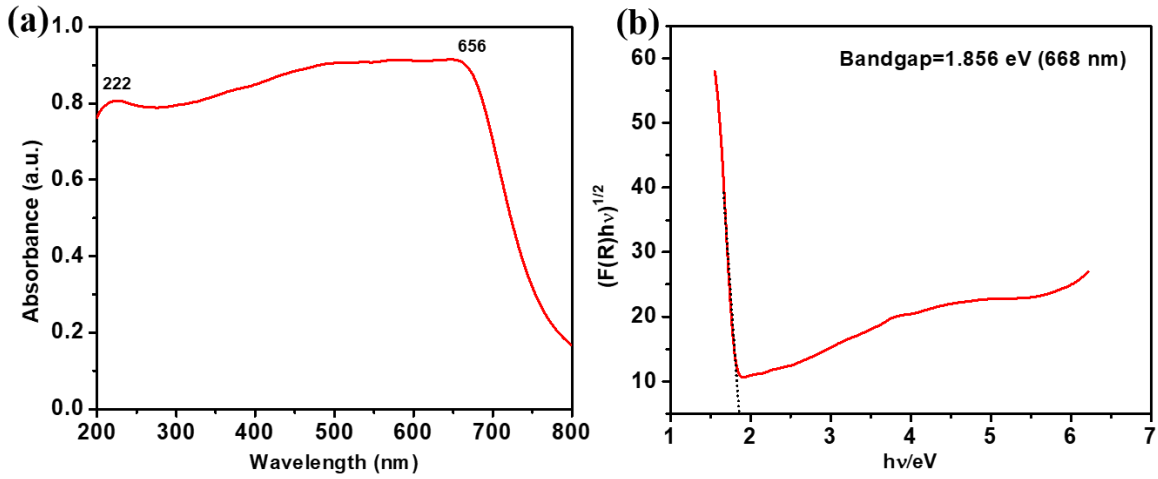

Fig.S5 (a) The absorption spectrum of bulk selenium powder sample collected at room temperature by UV-Vis diffuse reflectance spectroscopy (DRS). (b) Bandgap calculation from Tauc-plot.

The diffuse reflectance spectrum (DRS) of solid samples (as included in Fig. S5(a)) was collected using a spectrometer equipped with an integrating sphere. Barium sulphate (BaSO4) was used as the reference material. The absorption $\left(\frac{\alpha}{S}\right)$ data were calculated from the reflectance spectra using the Kubelka–Munk function: $\left(\frac{\alpha}{S}\right)=\frac{(1-R)^2}{2R}$; where R is the reflectance at a given wavelength, and α is the absorption coefficient, and S is the scattering coefficient. The UV-DRS spectrum of bulk selenium powder shows broadband absorption in the UV-Vis spectral range (200-700 nm).

V. Optimizing the choice of solvent for synthesizing selenium nanosheets

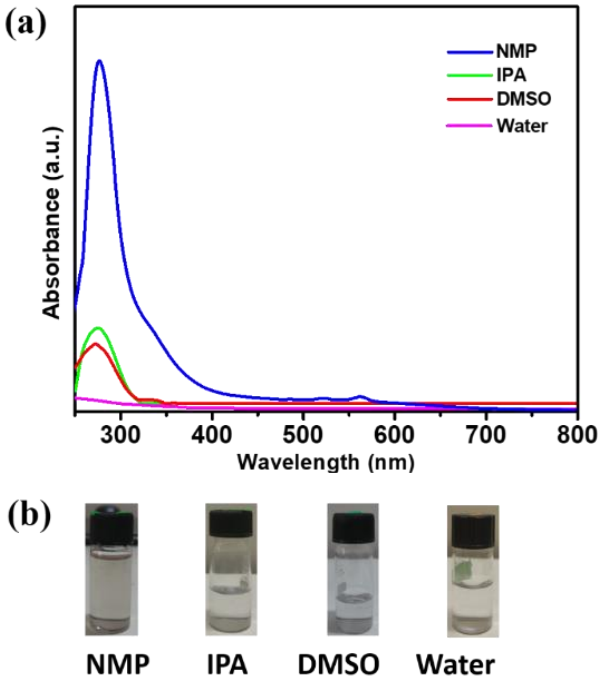

Fig.S6 (a) absorption spectra of samples prepared by stirring selenium powder in various solvents. (b) Digital photographs of the samples after centrifugation.

The solvents were used to prepare Se nanosheets, including N-methyl-2-pyrrolidone (NMP), water, and IPA. The bulk Se powder was added in the same concentration of 5 mg/ml for different solvents. Then, all the mixtures were bath-sonicated for 5 min and stirred for 24 hrs. Then they were centrifuged at 2000 rpm for 5 min. The supernatants in different solvents are shown in the above figure. The absorbance of the supernatants containing the synthesized

samples was then measured. It was discovered that Se nanosheets exfoliated in NMP could achieve a much higher absorbance, indicating a higher concentration of SeNS-1 compared to other counterparts.

VI. TEM images of selenium nanosheets

Fig.S7 (a) - (g) display the TEM images of SeNS-1 having the lateral size in the order of a few micrometres. Fig.S7 (h & i) demonstrate the HR-TEM images showing different d-spacings; inset (1), (2), and (3) imply d spacing of 0.15 nm, 0.13 nm, and 0.22 nm corresponds to (202), (113) and (110) lattice planes.

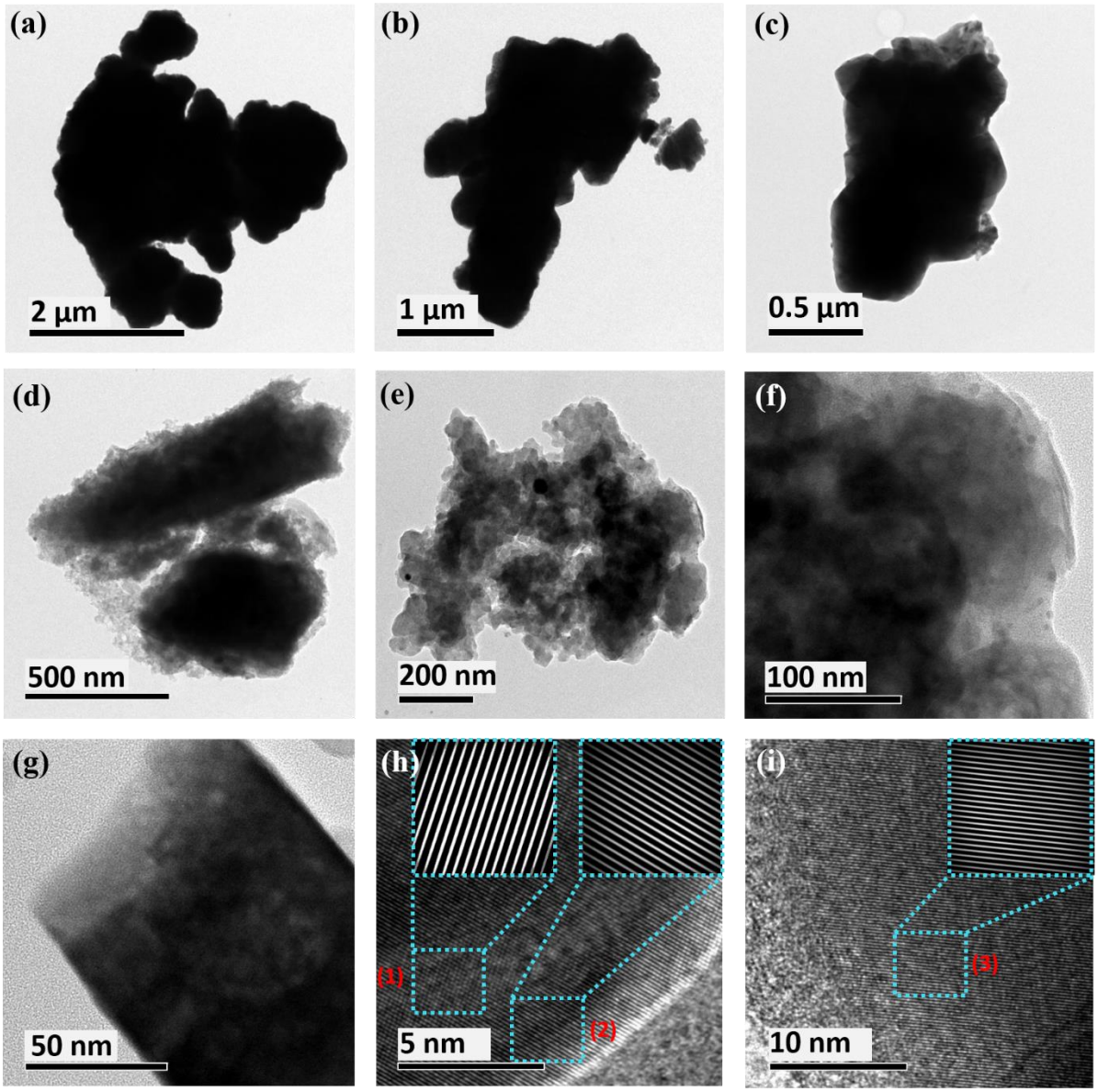

Fig.S7 (a)-(g) TEM images of SeNS-1 with a lateral size ranging from a few microns to hundreds of nanometers. (h) and (i) HRTEM images of SeNS-1.

VII. Indexing of SAED pattern

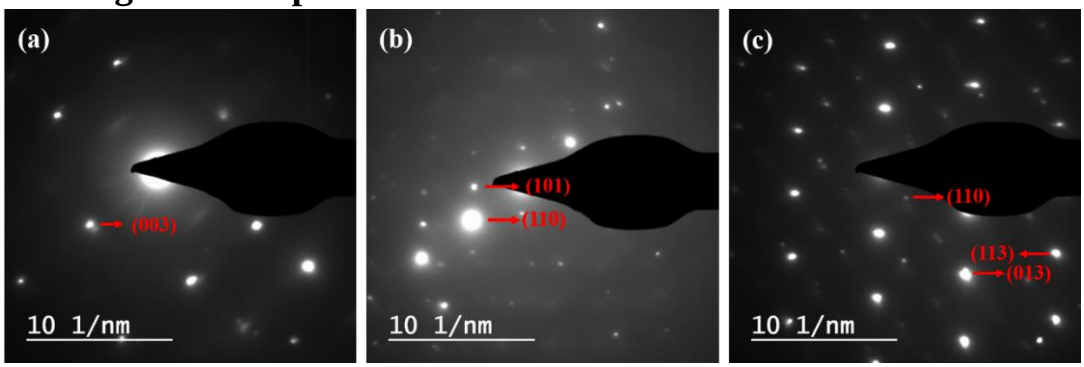

Fig.S8 SAED patterns obtained from SeNS-1. (a) selenium nanosheets show crystalline nature, and (hkl) values were assigned after calculating the d-spacings (Table.II) and matching those values with XRD

Fig. S5 (a)			Fig. S5 (b)			Fig. S5 (c)		
2D (nm^{-1})	d = 1/D (Å)	(hkl)	2D (nm^{-1})	d = 1/D (Å)	(hkl)	2D (nm^{-1})	d = 1/D (Å)	(hkl)
11.85	1.68	(003)	6.65	3.0	(101)	12.92	1.54	(013)
			8.76	2.2	(110)	15.15	1.32	(113)
						8.8	2.2	(110)

Table.II: Calculation of d-spacings from SAED patterns of SeNS-1. The (hkl) values were assigned after matching the d-values with XRD data.

VIII. Computational methodology

The alpha and beta (α and β) monolayers were obtained by cleaving the bulk unit cell along the (001) and (100) planes, respectively. A 25 Å vacuum was introduced along the z-direction to mitigate undesired interactions. The resulting lattice parameter for the α-selenene was determined to be 3.74 Å. The obtained lattice parameters for β-selenene are a = 4.19 Å and b = 5.00 Å which are in good agreement with previous results.[8] α-selenene is having a 1T-MoS_2 structure while β-selenene exhibits a tetragonal structure. In contrast to 1T-MoS_2, α-selenene exhibits two distinct types of Se atoms characterized by different coordination numbers. Specifically, a central Se atom situated at the Mo site displays a coordination number 6, whereas a Se atom within either the lower or upper layer, positioned at the S sites is a 3 coordinated one. In the case of β-Se, its structure comprises alternating arrangements of deformed four-membered and six-membered rings. The electronic band structures of the monolayers were analyzed by employing the hybrid HSE06 functional, which was performed as a single-shot calculation on top of the PBE structure. It was observed that both the α and β configurations exhibit semiconductor properties, each featuring an indirect band gap.

Specifically, the α configuration has an indirect band gap of 1.11 eV, while the β configuration possesses a larger indirect band gap of 2.59 eV. We could observe a decreasing trend in the band gap as we moved from the beta monolayer to the beta bilayer and trilayer configurations.

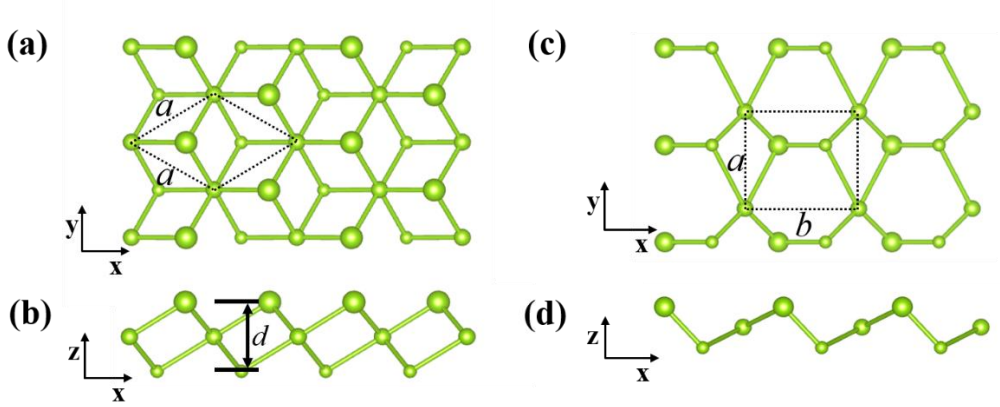

Fig.S9 The top and side views of monolayer of (a), (b) α-selenene and (c) and (d) β-selenene.

IX. XRD data and Raman spectra of SeNS-3 and SeNS-5

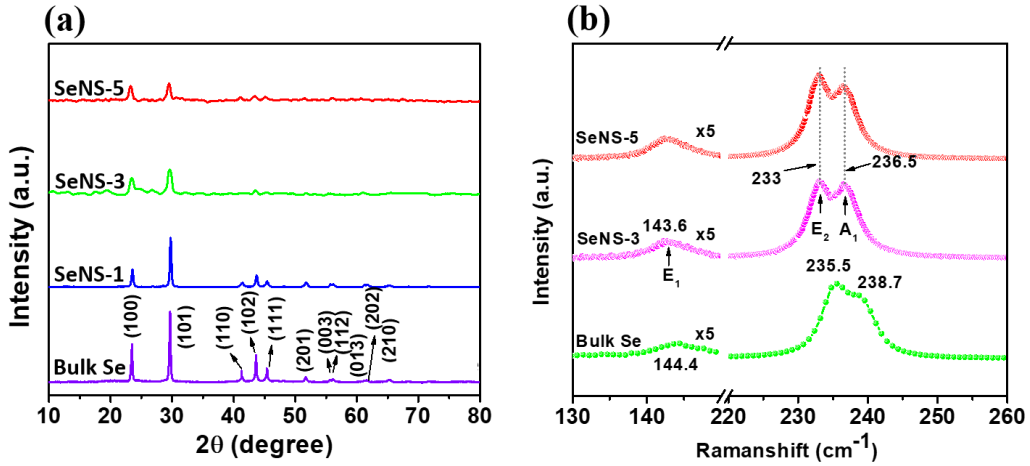

Fig.S10 (a) XRD data of Bulk Se, SeNS-1, SeNS-3 and SeNS-5 (b) Raman spectra of SeNS-3 and SeNS-5 with respect to bulk selenium.

Mode/Sample	E_1 (cm^{-1})	E_2 (cm^{-1})	A_1 (cm^{-1})
Bulk Se	144.4	235.5	238.7
SeNS-1	143.6	233.9	237.1
SeNS-1*	143.6	233.9	237.1
SeNS-3	143.6	233	236.5
SeNS-5	143.6	233	236.5

Table.III: Peak positions of Raman spectra of Bulk selenium, SeNS-1, SeNS-1*, SeNS-3 and SeNS-5**.**

X. Deconvolution of emission spectra

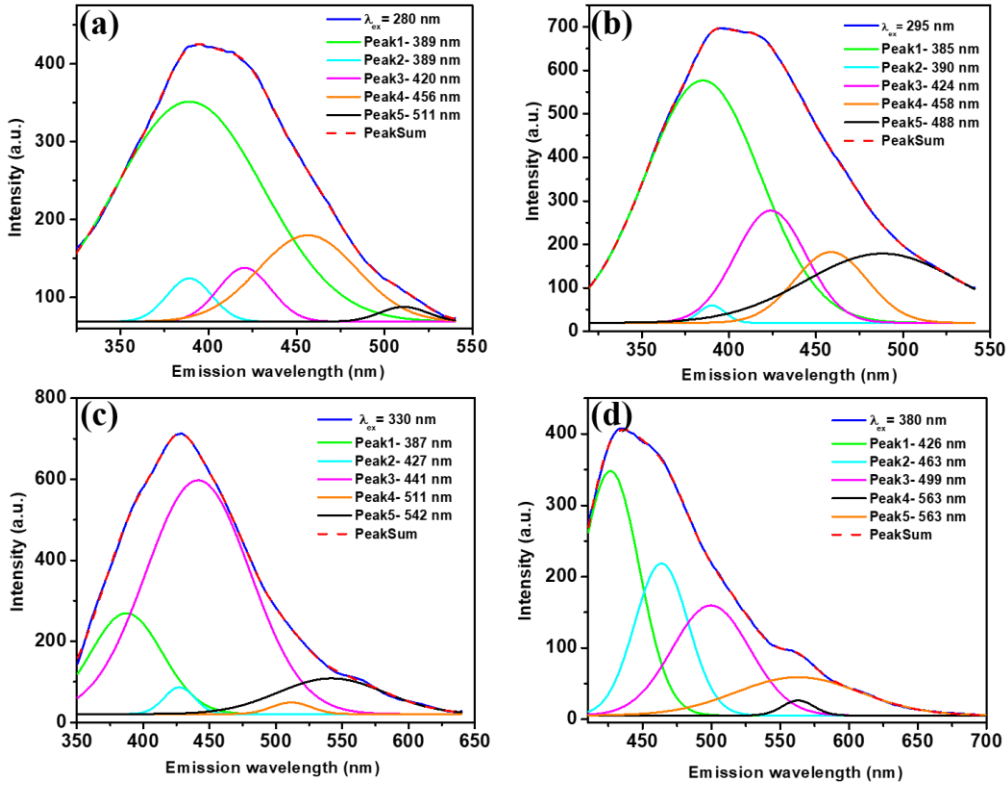

Fig.S11 Photoluminescence spectrum (blue line) recorded with excitation wavelengths of (a) 280 nm, (b) 295 nm, (c) 330 nm and (d) 380 nm. The deconvolution of the band gave five Gaussian components with peaks and the peak sum is shown by the dashed lines.

XI. Excitation spectra

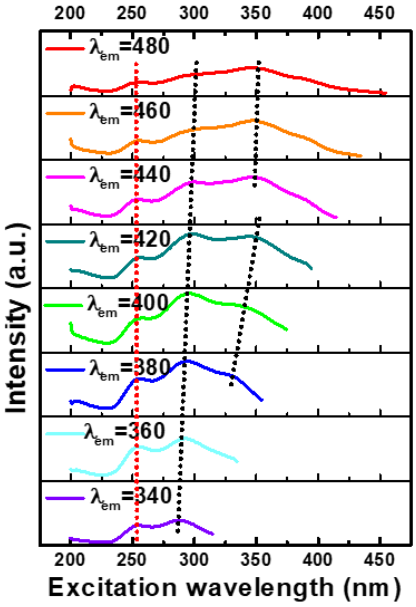

Fig.S12 Excitation spectra of SeNS-1 dispersed in NMP at emission wavelength range from 340 nm to 480 nm in 20 nm difference

XII. Emission spectra of SeNS-1 covering the entire emission band

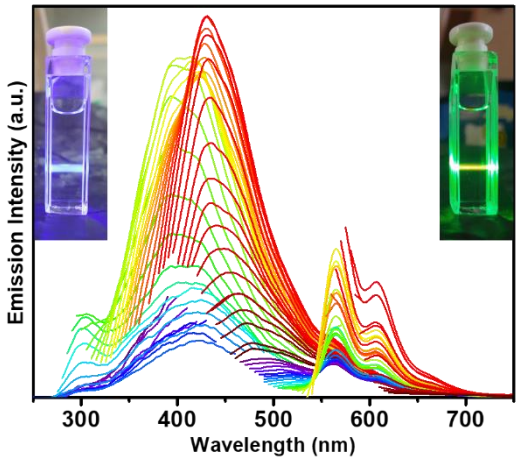

Fig.S13 Photoluminescence emission of SeNS-1 at the excitation wavelengths ranging from 200-600 nm in the step-size of 5 nm. Insets show optical emission at 450 nm (left) and 532 nm (right) excitation wavelengths.

XIII. Photoluminescence Quantum Yield (QY) measurements of SeNS-1 dispersion

The relative fluorescent quantum yield of SeNS-1 was calculated, taking quinine sulphate as a reference using the following equation.

$$QY_s = QY_{ref}\left(\frac{n_s}{n_{ref}}\right)^2 \frac{A_s F_{ref}}{A_{ref} F_s}$$

QY_s, n_s, A_s, F_s are the quantum yield, refractive index, absorbance, and integrated fluorescence intensity of the sample at $\lambda_{ex} = 310nm$ and $QY_{ref}, n_{ref}, A_{ref}, F_{ref}$ are the quantum yield, refractive index, absorbance, and integrated fluorescence intensity of the reference compound (quinine sulphate) at the excitation wavelength 310 nm. The quantum yield of the reference compound (quinine sulphate) was QY_{ref} ~ 0.546, and the ratio of the refractive indices was approximated as 1.22 in the calculation.

The Quantum Yield (QY) of the SeNS-1 dispersion

$$QY = 0.546 \times 1.22 \times \frac{0.0304}{0.0903} \times \frac{17318}{35737} = 0.1088 = 10.88\%$$

XIV. Electronic Band structures and Optical Response of α-selenene and β-selenene

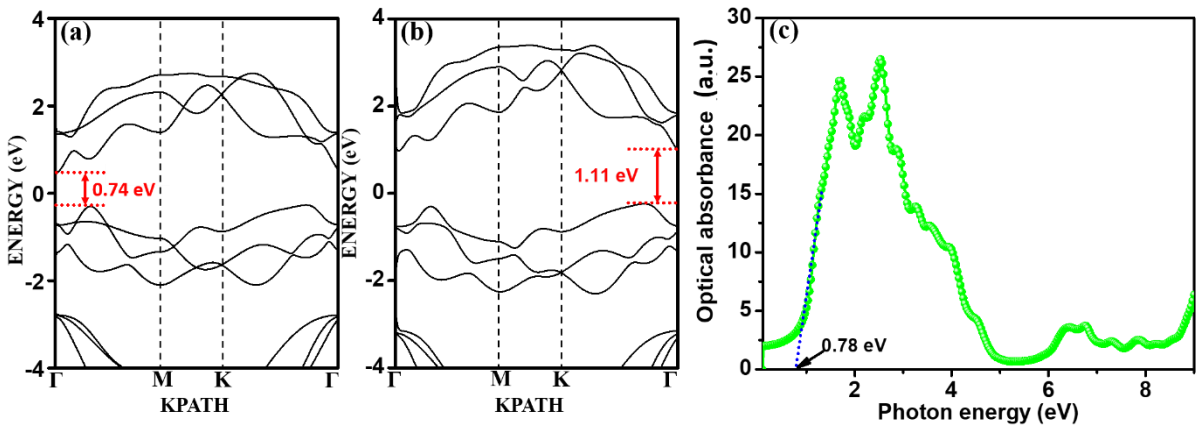

Fig.S14 Band structures of monolayer of α-Se (a) with PBE functional (b) with HSE06 exchange-correlation functional (c) Optical absorbance of monolayer of α-Se with PBE functional.

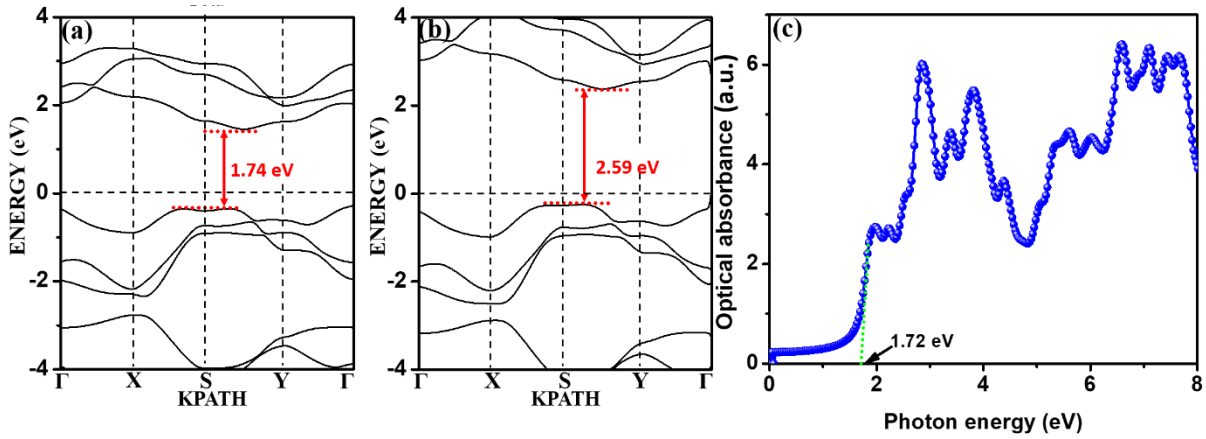

Fig.S15 Band structures of the monolayer of β-Se (a) with PBE functional (b) with HSE06 exchange-correlation functional (c) Optical absorbance of monolayer β -Se with PBE functional.

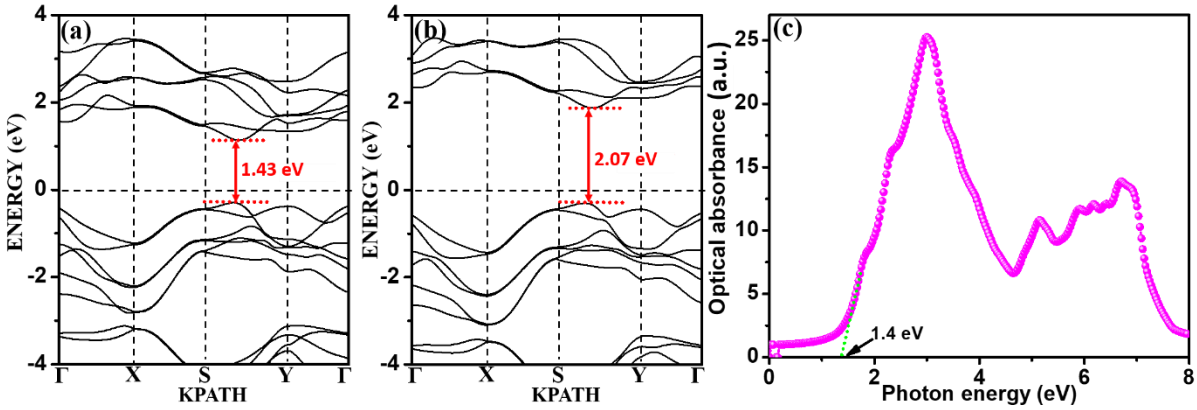

Fig.S16 Band structures of bilayer of β -Se (a) with PBE functional (b) with HSE06 exchange-correlation functional (c) Optical absorbance of bilayer β -Se with PBE functional.

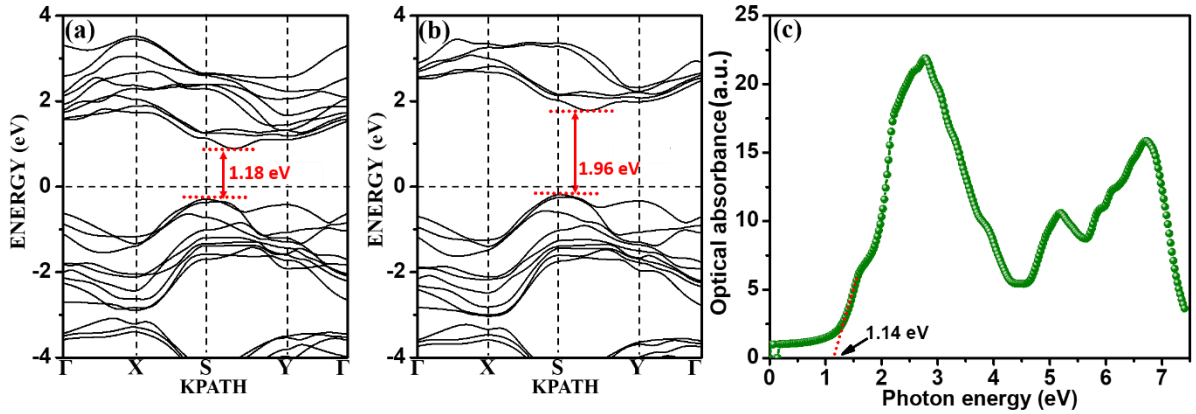

Fig.S17 Band structures of trilayer of β -Se (a) with PBE functional (b) with HSE06 exchange-correlation functional (c) Optical absorbance of trilayer β -Se with PBE functional.

XV.Excitation-emission matrix of Bulk Selenium powder

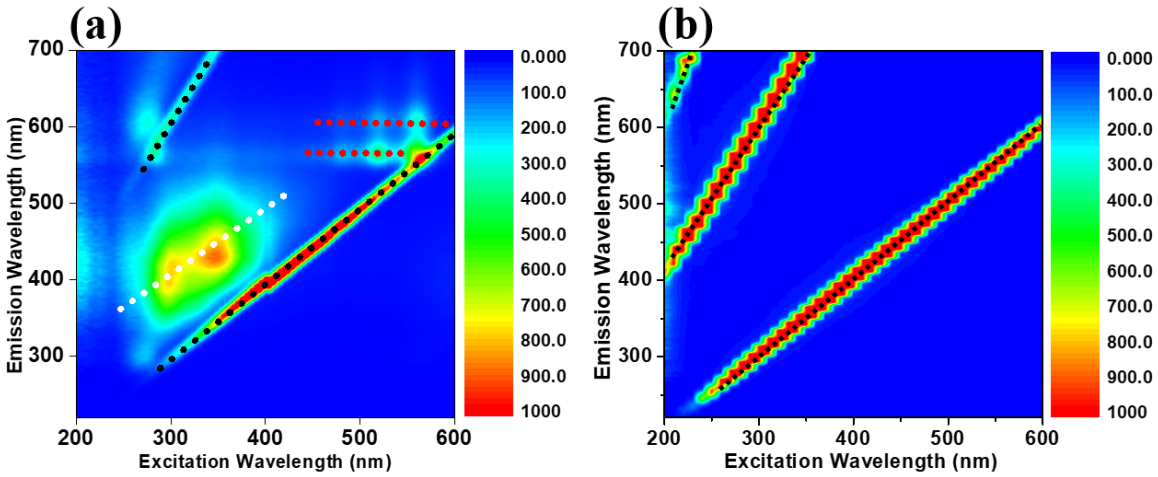

Fig.S18 Contour plot obtained from the excitation-emission matrix of (a) SeNS-1 dispersion in NMP (b) bulk selenium powder covering the excitation wavelength from 200-600 nm

The contour plot obtained from the excitation-emission matrix did not show any significant emission behaviour, apart from first-order, second-order, and third-order harmonic peaks, denoted by black dotted lines.

XVI. Lifetime measurements via Time-Correlated Photon Counting (TCSPC)

The photoluminescence decay curves were fitted using a three-exponential function using the equation

$$I(t) = A_1 e^{\frac{-t}{\tau_1}} + A_2 e^{\frac{-t}{\tau_2}} + A_3 e^{\frac{-t}{\tau_3}}; A_1 + A_2 + A_3 = 1$$

τ_1, τ_2, τ_3 are the decay time constants and A_1, A_2, A_3 represent the normalized amplitudes of each component. The average lifetime of the photoluminescence decay process was determined using the equation

$$\tau_{avg} = \frac{A_1\tau_1^2 + A_2\tau_2^2 + A_3\tau_3^2}{A_1\tau_1 + A_2\tau_2 + A_3\tau_3}$$

The decay parameters of the dispersion of SeNS-1 in NMP estimated from the TCSPC data are given in Table.IV.

λ_{ex} (nm)	$\tau_1(ns)$	$\tau_2(ns)$	$\tau_3(ns)$	A_1	A_2	A_3	τ_{avg}
295	6.86	34.47	1.43	45.74	34.64	19.62	28 ns
330	6.62	41.61	1.29	41.69	25.27	33.04	33 ns
570	3.73	17. 1		99.26	0.74		41 ps

Table.IV: The fitting parameters for the photoluminescence decay curves.

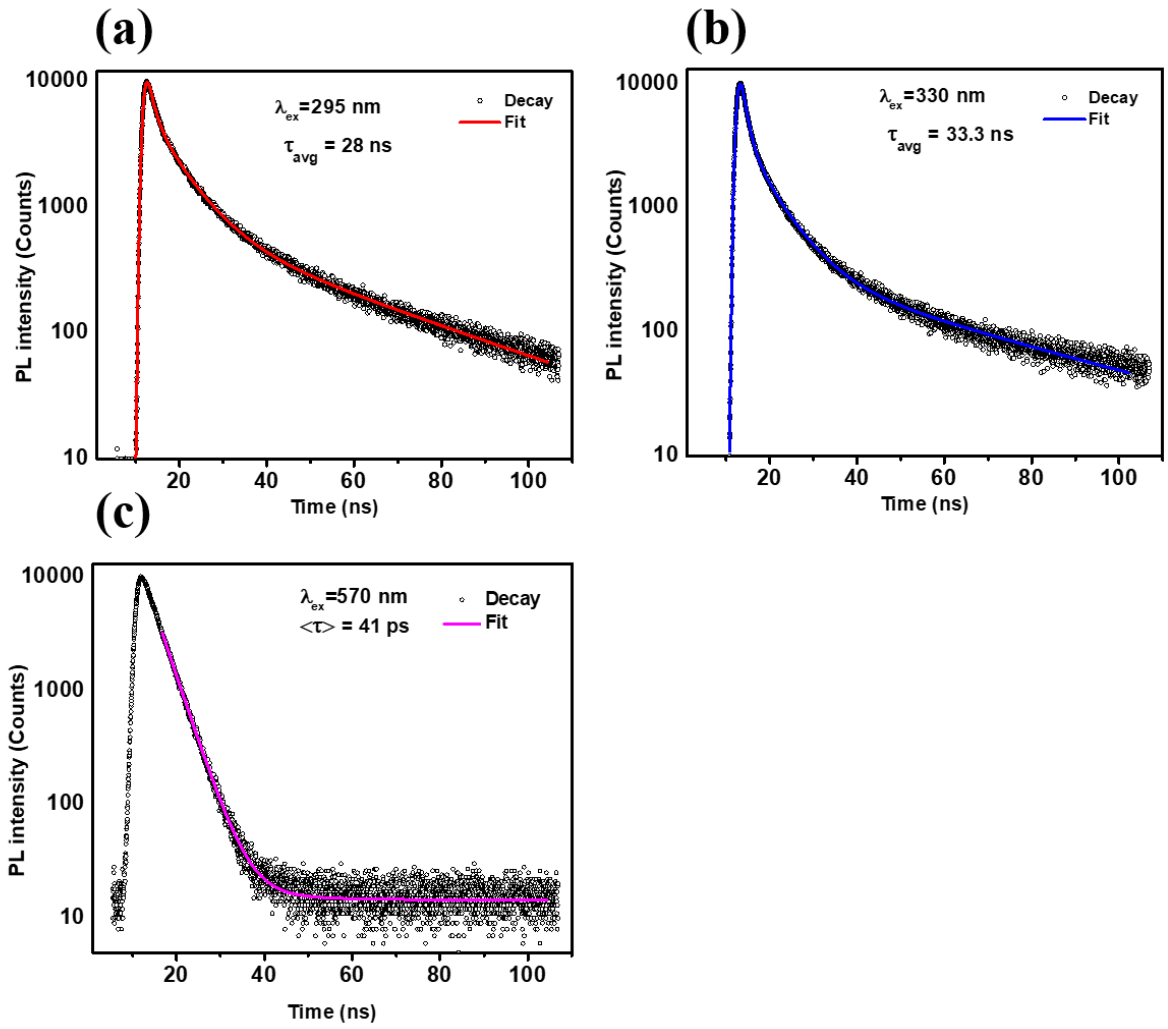

Fig.S19 Photoluminescence decay of SeNS-1 dispersed in NMP at (a) λ_{em} = 400 nm, (b) 420 nm and (c) 608 nm.

XVII. Energy level diagram

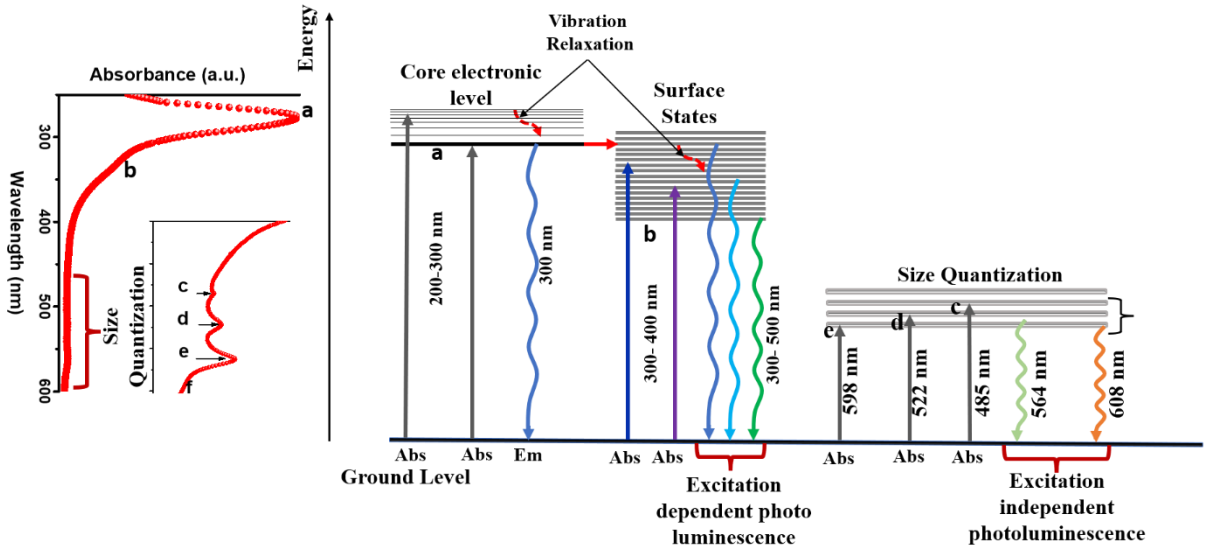

Fig.S20 The proposed schematic diagram represents the energy levels and the electronic transitions in the SeNS-1.

XVIII. Absorption spectra of selenium nanosheet dispersions stirred at different times.

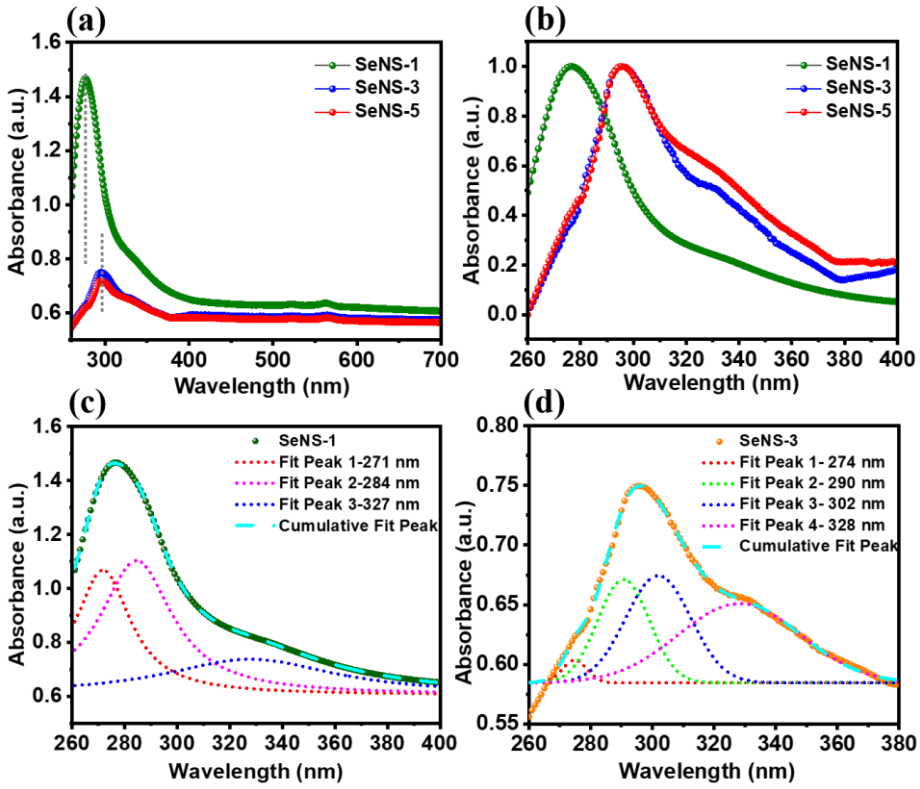

Fig.S21 (a) UV-Vis absorption spectra of SeNS-1, SeNS-3 and SeNS-5. (b) Normalized absorption spectra of the same. Deconvolution of absorption spectra of (c) SeNS-1 and (d) SeNS-3.

	β_{NL} (cm/GW)	I_s (GW/cm^2)
SeNS-1 day	30	4.49
SeNS-3 days	0.005	0.0399
SeNS-5 days	0.001	0.0399

Table.V: Z-scan parameters for selenium nanosheet dispersions in NMP

References

1 G. Kresse and J. Furthmüller, *Phys. Rev. B*, 1996, **54**, 11169–11186.

2 G. Kresse and J. Hafner, *Phys. Rev. B*, 1993, **47**, 558–561.

3 J. P. Perdew, K. Burke and M. Ernzerhof, *Phys. Rev. Lett.*, 1996, **77**, 3865–3868.

4 S. GRIMME, Semiempirical GGA-Type Density Functional Constructed with a Long-Range Dispersion Correction, *Wiley Intersci.*, 2006, **27**.

5 J. Heyd, G. E. Scuseria and M. Ernzerhof, *J. Chem. Phys.*, 2003, **118**, 8207–8215.

6 P. E. Blöchl, *Phys. Rev. B*, 1994, **50**, 17953–17979.

7 J. D. Pack and H. J. Monkhorst, *Phys. Rev. B*, 1977, **16**, 1748–1749.

8 D. Wang, L. M. Tang, X. X. Jiang, J. Y. Tan, M. D. He, X. J. Wang and K. Q. Chen, *Adv. Electron. Mater.*, 2019, **5**, 1–6.